Mechano-calcium and mechano-electric feedbacks in the human cardiomyocyte analyzed in a mathematical model

Nathalie A. Balakina-Vikulova[1,2] • Alexander Panfilov[2,3] • Olga Solovyova[1,2] • Leonid B. Katsnelson[1,2]

Received: … / Accepted: … / Published online: … © … 2019

Abstract

Experiments on animal hearts (rat, rabbit, guinea pig, etc.) showed that mechano-calcium feedback (MCF) and mechano-electric feedback (MEF) are very important for myocardial self-regulation. This is because they adjust cardiomyocyte contractile function to various mechanical loads and to the mechanical interaction of heterogeneous myocardial segments in the ventricle walls. In the *in vitro* experiments on these animals MCF and MEF manifested themselves in several basic classic phenomena (e.g. load dependence, length dependence of isometric twitches, etc.), and in the respective responses of calcium transients and action potentials. However, simultaneous study of electrical, calcium, and mechanical activity of the human heart muscle *in vitro* is extremely difficult. Here we apply mathematical modeling to study these phenomena. We develop a novel model describing electromechanical coupling and mechano-electric feedbacks in the human cardiomyocyte. This model combines the 'ten Tusscher – Panfilov' electrophysiological model of the human cardiomyocyte with our module of the myocardium mechanical activity taken from the 'Ekaterinburg – Oxford' model and adjusted to human data. Using it we model isometric and isotonic twitches and study effects of MCF and MEF on the excitation-contraction coupling. We have shown that MCF and MEF both for smaller afterloads as compared to bigger ones and for various mechanical interventions during isometric and isotonic twitches substantially affect durations of calcium transient and action potential in the human cardiomyocyte model.

Keywords

Human myocardium · Electromechanical coupling · Mechano-electric feedback

1 Introduction

Although the main function of electrical excitation in the heart is to initiate mechanical contraction, mechanical contraction also affects electrical wave propagation via processes called mechano-calcium feedbacks (MCF) and mechano-electric feedbacks (MEF) [1-3]. Physiological role of the influence of mechanical conditions on the activity of the heart muscle is manifested, in particular, in adaptation of normal myocardium to varying external and internal mechanical conditions of contraction, including global and local mechanical loading and length redistribution between interacting heterogeneous cardiomyocytes in the heart chamber walls [4]. Differing in the durations of the twitch, in the ability for the mechanical tension development, and being excited with a delay relatively to each other, the interacting myocardial cells produce dynamically changing conditions of the mechanical loading for each other. As a result, a complex continuous chain of feedbacks (MEF and MCF) arises between the contraction of the whole ensemble of the cardiomyocytes in the wall and activation of each of them. In turn, these feedbacks dynamically modulate subsequent course of the twitch for each of them. We have earlier studied these effects experimentally on the simplest biological models that reflect such interactions: on heterogeneous muscle duplexes [5-8], as well as on mathematical models of such duplexes, and on one-dimensional models of cardiac heterogeneous tissue [5, 6, 8-10].

On the other hand, the pathological manifestations of these feedbacks can be quite dramatic: for example, they can cause heart rhythm disturbances and even lead to sudden cardiac death [1]. The experimental data on the electromechanical activity are mainly collected in animal heart; however, data for the human cardiomyocyte are very limited. Also mechanisms behind MCF and MEF are not fully understood.

In particular, there are several intracellular mechanisms shown to contribute to the cardiac MCF. Mechano-dependence of sarcoplasmic reticulum Ca^{2+} spark rate may contribute to the MCF via the calcium induced calcium release [11]. A key circuit of the MCF is associated with the load and/or length dependent kinetics of the calcium-troponin C (TnC) complexes regulating Ca^{2+} activation of the cardiomyocyte contractions [12, 13].

[1] Institute of Immunology and Physiology of the Ural Branch of the Russian Academy of Sciences, Ekaterinburg, Russia
[2] Ural Federal University, Ekaterinburg, Russia
[3] Ghent University, Ghent, Belgium

MCF contribute to both fast and slow force responses of the heart muscle to stretches and other types of deformation. Moreover, MCF can trigger MEF, since mechano-dependent modulation of the shape and duration of the calcium transient during mechanical twitch can affect the shape and duration of the action potential via Ca^{2+} currents including Na^{+}-Ca^{2+} exchange current.

Another mechanism of the MEF is related to the activity of mechano-sensitive ion channels in the cardiomyocyte membrane [14]. While contribution of these channels to MEF is generally recognized, many details remain poorly understood, including the characteristics of their conductivity response to the stretch, their localization in the cell membrane and ionic specificity. There are reasons to believe that contribution of the stretch-activated ion channels to the myocardium mechanical activity is manifested more likely in slow force response effects rather than in the fast ones (see Discussion). Meanwhile, in this work we focus mainly on the fast force response phenomena listed below.

In experiments on isolated cardiac muscle preparations (trabeculae and papillary muscles) from the hearts of the animals (rat, rabbit, guinea pig, etc.) the MCF and MEF were revealed as the following basic classic phenomena: length dependence of isometric twitches, load dependence of isotonic contractions, muscle inactivation due to short-time deformations during isometric twitches (see [15] for a review), and in the respective responses of calcium transients and action potentials on the mechanical interventions. Such integrative data were purely reported for the human cardiac preparations, while plural clinical evidence for contraction-excitation feedback in humans, mechano-dependent arrhythmias included is published [1, 16, 17].

The main goal of this paper is to predict possible MCF and MEF manifestations in a human cardiac muscle using modeling. For that, we develop a novel mathematical electromechanical model by integrating limited experimental data on excitation-contraction and mechano-electrical coupling in healthy and pathological human myocardium. Using it, we study MCF and MEF manifestations. The developed electromechanical model of human cardiomyocytes is also by itself an important result as it can be used to study electromechanical effects in myocardial tissue and the whole human heart for diagnosis and effective treatment of cardiac diseases.

Several models of the human cardiomyocytes describe electrophysiological function of the cells [18-21]. However, only in few cases these models are combined with cardiac mechanics [22-25]. The question on the presence of MEF in human cardiomyocytes was raised in the recent work [24], where two human electrophysiological models [19, 21] were combined with mechanical models developed by J. Rice [26] and by S. Land [27]. The authors parametrically fitted the Rice model for the human cardiomyocyte whereas the Land model was specially developed to simulate contractions and passive viscoelasticity in human cardiomyocytes. In the case of the Land model, MCF in electromechanical models was inherited from the Rice model as well. The authors did not find MEF in any of the considered electromechanical models. Therefore, they have concluded that MEF seems not to be present in the healthy human myocardium. However, this conclusion is based on the specific features of MCF of Rice model [26] which may be not properly describe a wide range of important mechanics effects In the 'Discussion' section we will characterize in more detail some important distinctions between our approach and that suggested in the Rice model resulting in different mechano-sensitivity of the cardiomyocyte calcium activation.

Experimental studies proved that MEF exists in myocardium from the cellular to organ level in many species of mammals, and manifests itself in the intact human hearts *in vivo*. Thus, we believe that this property should also be present in the human myocardial cells and plays an important physiological/pathophysiological role in regulation of the human heart function. In the paper, we develop a novel electromechanical model (TP+M) based on combination of the electrophysiological model and the model of the cardiomyocyte mechanics [28]. Using it, we evaluate MCF and MEF manifestations in the human cardiac cells.

2 Methods

2.1 TP+M model

The combined model of the excitation-contraction coupling (ECC) in the human cardiomyocyte (TP+M model) is formed of two main modules: electrophysiological and mechanical parts coupled to each other.

The module for cellular electrophysiology is based on the 2006 version of 'ten Tusscher – Panfilov' (TP) ionic model, which is described in detail elsewhere [20] and has been widely used in electrophysiological studies [29-32]. The TP model describes ionic currents across the membrane and generation of the action potential (AP) (see Fig. 1 for details). Particularly, this model was used as the electrical component in electromechanical models combined with different mechanical modules [22, 23, 33].

The module of the mechanical activity has been developed by us earlier and used as a component in the electromechanical model 'Ekaterinburg – Oxford' [28] describing ECC in the cardiomyocytes of various animals (e.g.

guinea pig and rabbit), adapted to each particular species via a parameter tuning.

The rheological scheme of this module is presented in Fig. 2. The mechanics of passive elastic and viscous elements, as well as the mechanical activity of the contractile element are described by a system of ordinary differential and algebraic equations we published earlier [28]. The only difference with that our work is in usage now of two viscous elements to keep simulation of cardiac biomechanical effects observed experimentally. As we had shown even earlier as compared to the cited article by Sulman et al. the second viscous element (see Fig. 2) is responsible for the experimentally observed time lag between the duration of the muscle force increase phase and the duration of the sarcomere shortening during isometric twitches [34]. This property turns out quite useful for the fitting of the time-to-peak isometric force to the range of the experimentally observed values (see below). In other words, in the article by Sulman et al. the second viscous element was eliminated only for simplifying the model; however in the case when the model should simulate quantitative species-specific features of the contractile cycle, this element cannot be neglected.

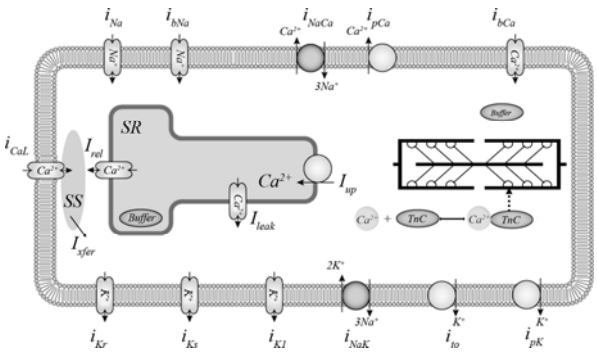

Fig. 1 Ionic membrane currents and intracellular calcium homeostasis in the TP+M model. **Calcium currents**: i_{CaL} – L-type Ca^{2+} current; i_{bCa} – background Ca^{2+} current. **Potassium currents**: i_{K1} – inward rectifier K^+ current; i_{to} – transient outward current; i_{Kr}, i_{Ks} – rapid and slow delayed rectifier current; i_{pK} – plateau K^+ current. **Sodium currents**: i_{Na} – fast Na^+ current; i_{bNa} – background Na^+ current. **Pumps and exchangers**: i_{pCa} – sarcolemmal Ca^{2+} pump current; i_{NaK} – Na^+-K^+ pump current; i_{NaCa} – Na^+-Ca^{2+} exchanger (NCX) current. **Calcium translocations**: I_{rel} – Ca^{2+} release from the sarcoplasmic reticulum (SR) via ryanodine receptors to the subspace (SS); I_{xfer} – Ca^{2+} diffusion from SS to the cytoplasm; I_{leak} – a small Ca^{2+} leakage from the SR to the cytoplasm; I_{up} – Ca^{2+} pumping from the cytoplasm to the SR, where Ca^{2+} partially buffered (*Buffer* in SR). Cytoplasmic buffering is divided into two compartments: Ca^{2+}-troponin C complexes formation (*Ca-TnC*) inherited from [28] and buffering by other intracellular ligands (*Buffer*). The figure is modified from the diagram in the Physiome Model Repository[4] based on [20].

The main component of this scheme is a contractile element, representing sarcomeres in the cardiomyocyte. This element is responsible for both generation of the active force developed by the cardiomyocyte and its shortening due to the cross-bridges (Xb-s) formed by myosin heads attached to the actin thin filaments. Xb attachment during the contractile cycle is regulated by Ca^{2+} ions through their binding to TnC located along the thin filament. Differential equations describing Xb kinetics and Ca^{2+}-troponin C complex (Ca-TnC) kinetics in the model are provided in the Supplement.

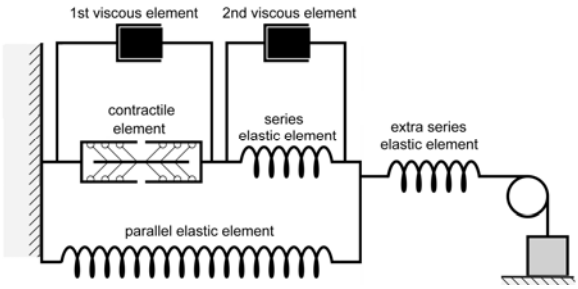

Fig. 2 Rheological scheme of virtual cardiac sample in the TP+M model. It consists of a contractile element, which is a generator of active force, three elastic and two viscous elements. Contractile element in the model reproduces sarcomeres in the cardiomyocyte

An important feature of this model is a mathematical description of the mechanisms of cooperativity [28], which make the kinetics of Ca-TnC dependent on the number of attached force-generating Xb-s. In particular, the decay of the Ca-TnC complex becomes slower if the larger number of Xb-s binds to actin and/or if the larger number of other Ca-TnC complexes are formed along the thin filament near it.

Cooperative effects of the attached Xb on the Ca-TnC kinetics contribute to the MCF in the 'Ekaterinburg – Oxford'

[4] https://models.physiomeproject.org/exposure/a7179d94365ff0c9c0e6eb7c6a787d3d/ten_tusscher_model_2006_IK1Ko_M_units.cellml/view

model via the length dependence of the Xb attachment/detachment in the model.

Particular mechanisms underlying the length effects on the Xb attachment are being extensively debated. For a long time, the lattice spacing concept was prevailing one, suggesting that a decrease in the sarcomere inter-filament distance due to the cardiomyocyte lengthening facilitates actomyosin interactions and thus increases the probability of the Xb attachment [35, 36]. Recent experimental studies unraveled an essential role of the giant protein titin in the length dependence of the Xb dynamics [37, 38]. In the 'Ekaterinburg – Oxford' model, the length dependent probability for Xb binding is described phenomenologically as an overall result of all possible underlying molecular mechanisms. Thus, this formalization is invariant with respect to the discussed fine mechanisms. Together with the above cooperativity, this length dependent probability allows the 'Ekaterinburg – Oxford' model to reproduce most of the MCF and MEF effects found in the heart muscle.

The cooperativity of Ca^{2+} myofilament activation in the mechanical module has allowed the 'Ekaterinburg – Oxford' model to reproduce a wide range of experimental manifestations of the effects of mechanical conditions of cardiac muscle contraction on the intracellular calcium kinetics (in particular, the effect of its shortening). Moreover, this MCF allows the 'Ekaterinburg – Oxford' model to reproduce effects of contraction on the cellular electrical activity, particularly on the shape and duration of AP [9, 28]. It was found that Ca^{2+}-dependent modulation in the Na^{+}-Ca^{2+} exchange (NCX) current of the Noble'98 ionic model [39] triggers MEC in the combined 'Ekaterinburg – Oxford' model [9, 28].

The TP ionic model and the Ekaterinburg mechanical model are coupled and form the TP+M model via Ca^{2+} handling. However, description of such coupling required some model modification. In particular, TP model does not describe the Ca-TnC kinetics. It contains a mathematical description of only a generalized calcium-binding buffer in cytosol, simulating overall contribution of calcium-binding intracellular ligands and TnC. Moreover, a quasi-stationary algebraic equation is used to describe this cytosolic Ca^{2+} buffering in the TP model.

However, the Ca-TnC kinetics is essential for initiation of the contraction, and therefore is described in the Ekaterinburg mechanical model by an ordinary differential equation separately from other intracellular Ca^{2+} binding ligands. Moreover, the cooperative mechanisms of MCF linking the Ca-TnC and Xb kinetics are described in the corresponding differential equations in the mechanical module of the Ekaterinburg model. These cross-links are the key mechanisms of cardiac ECC, which have to be reflected in our new model and will be used to evaluate a degree of MCF and MEF manifestations in the human cardiac cells.

Thus, in the combined TP+M model, we introduced a separate differential equation for Ca-TnC kinetics similar to that of the Ekaterinburg mechanical module and re-fitted the parameters in the algebraic quasi-stationary equation for the generalized calcium buffer of the TP model.

In addition, we have changed some parameter values in the equation for the NCX current (i_{NaCa}) from the TP model to fit the combined TP+M model to experimental data. Details of this parametric tuning are described below.

All the equations and parameters of the combined TP+M model are presented in the Supplement. Here we provide only equations of the of Ca^{2+} handling module, which were modified in the TP+M model compared to the TP model.

The following equation describes the time-dependent changes in the Ca-TnC concentration ($[Ca\text{-}TnC]$) [28]:

$$\frac{d[Ca\text{-}TnC]}{dt} = a_{on} \cdot (TnC_{tot} - [Ca\text{-}TnC]) \cdot [Ca^{2+}]_i - a_{off} \cdot e^{-k_A \cdot [Ca\text{-}TnC]} \cdot \Pi(N) \cdot [Ca\text{-}TnC], \quad (1)$$

where TnC_{tot} is the total concentration of TnC in cytosol; $\Pi(N)$ is the cooperative dependence of dissociation of Ca-TnC complexes on the Xb concentration N; a_{on}, a_{off}, k_A are model parameters (see the Supplement for details).

Mechanisms of cooperativity are described in detail in our previous works [28, 40, 41].

The following equation describes the time-dependent changes in free intracellular Ca^{2+} concentration ($[Ca^{2+}]_i$):

$$\frac{d[Ca^{2+}]_i}{dt} = Ca_{i_{bufc}} \cdot \left(\frac{(I_{leak} - I_{up}) \cdot V_{SR}}{V_c} + I_{xfer} - \frac{(i_{bCa} + i_{pCa} - 2 \cdot i_{NaCa}) \cdot C_m}{V_c \cdot F} - \frac{d[Ca\text{-}TnC]}{dt} \right). \quad (2)$$

Here, the first term describes Ca^{2+} release (I_{up}) and leakage (I_{leak}) from and Ca^{2+} SERCA uptake (I_{up}) to the of sarcoplasmic reticulum (V_c is the cytoplasmic volume, V_{SR} is the SR volume). The second term (I_{xfer}) refers to the Ca^{2+} diffusion leakage from the subspace into the cytoplasm. The third term describes Ca^{2+} currents through the cell membrane (F is the Faraday constant, C_m is the membrane capacitance). The descriptions of fluxes and ion currents are inherited from the TP model. The term $\frac{d[Ca\text{-}TnC]}{dt}$ accounts for Ca^{2+} binding to TnC as provided by the Eq. 1.

The factor $Ca_{i_{bufc}}$ is derived from the quasistationary formulation for the overall concentration of Ca^{2+} bound to intracellular buffer ligands other than troponin C in the TP model:

$$Ca_{i_{bufc}} = \frac{1}{1 + \frac{Buf_c \cdot K_{bufc}}{([Ca^{2+}]_i + K_{bufc})^2}}, \tag{3}$$

where Buf_c is the total concentration of all calcium-binding buffer proteins in the cytoplasm except TnC, K_{bufc} is the half-saturation constant for the generalized Ca^{2+} buffer.

The description of the generalized buffer given by Eq. 3 from the TP model. We have changed parameters in Eq. 3 to fit the sum of the modified calcium-buffer concentration and *[Ca-TnC]* in the combined TP+M model to the overall calcium-buffer concentration in the original TP model.

The following formulation for the NCX current is also taken from the TP model:

$$i_{NaCa} = \frac{K_{NaCa} \cdot (e^{\frac{\gamma \cdot V \cdot F}{R \cdot T}} \cdot [Na^+]_i^3 \cdot [Ca^{2+}]_o - e^{\frac{(\gamma-1) \cdot V \cdot F}{R \cdot T}} \cdot [Na^+]_o^3 \cdot [Ca^{2+}]_i \cdot \alpha)}{(Km_{Nai}^3 + [Na^+]_o^3) \cdot (Km_{Ca} + [Ca^{2+}]_o) \cdot (1 + K_{sat} \cdot e^{\frac{(\gamma-1) \cdot V \cdot F}{R \cdot T}})}, \tag{4}$$

where V is the membrane potential, γ is the parameter of the dependence of the NCX current on the potential; $[Na^+]_i$, $[Ca^{2+}]_i$, $[Na^+]_o$, $[Ca^{2+}]_o$ are intracellular and extracellular concentrations of Na^+ and Ca^{2+}; K_{NaCa} is the maximum NCX current; Km_{Ca} is the saturation constant for Ca^{2+}; Km_{Nai} is the saturation constant for Na^+; K_{sat} is the saturation coefficient for the NCX current at very negative potentials; α is a multiplier due to which one can increase the contribution of the term responsible for the inwardly directed current; R is the gas constant; F is the Faraday constant; T is the temperature.

2.2 Simulation design and protocols

The main goal of this paper is to analyze possible effects of MCF and MEF in the human myocardium in various modes of contraction. For that, we carried out three types of tests with the virtual preparation, presented by the TP+M model: (1) various loading modes applied to the contracting virtual sample; (2) different initial lengths of the virtual sample, i.e. different preloads; (3) quick changes in length during the sample contractions. The TP+M model is used to simulate these various modes of myocardial contraction.

As we mentioned in the Introduction, experimental data on the mechanical activity in cellular or multicellular human myocardial preparations are very limited. In few experimental works performed in the nineties of the 20th century, contraction of papillary muscle and trabeculae from the ventricles of the human hearts were studied in isometric mode [42-57] and only two papers report on contractions under mechanical loads [47, 55]. Below, in our simulations we compare, wherever possible, the data of numerical experiments with the results from the listed works. However, in those studies, action potentials (APs) were not recorded during muscle contractions. On the other hand, the protocols of all our numerical experiments reproduce protocols implemented in various animals experiments used to quantify MCF and MEF. Therefore, all phenomena we model are also compared qualitatively with data from these studies on animals, including mechanical recordings, Ca^{2+} transients in cardiomyocytes and APs.

Simulated signals generated by the TP+M model in the isometric mode of contraction are shown in the steady-state for the pacing rate of 1 Hz. The simulated responses to mechanical interventions (e.g. change in the imposed external load (afterload), quick stretch, and quick release) are evaluated during the first twitch where the intervention is applied accordingly to experimental protocols [41, 55, 58, 59].

Thus, our study is focused on the analysis of the fast (immediate) responses of the human myocardium to the mechanical exposures.

3 Results

3.1 Mechano-calcium and mechano-electric feedbacks arising in response to different loading modes

3.1.1 Simulation of isotonic afterloaded twitches

We start with simulation of the effect of load dependent relaxation, which most clearly demonstrates the influence of myocardial contraction on its electrical activation. More than forty years ago this effect was shown for the first time in experiments on papillary muscles and trabeculae of mammals and frogs, and revealed the higher velocities of the muscle lengthening (relaxation) in isotonic twitches under the smaller loads than under the larger ones [60, 61]. This paradoxical effect indicated inactivation of the muscle contractility due to the reducing of the applied load. Later this effect was

confirmed in various experimental studies on various mammals – rat, rabbit, cat, etc [41, 58, 59].

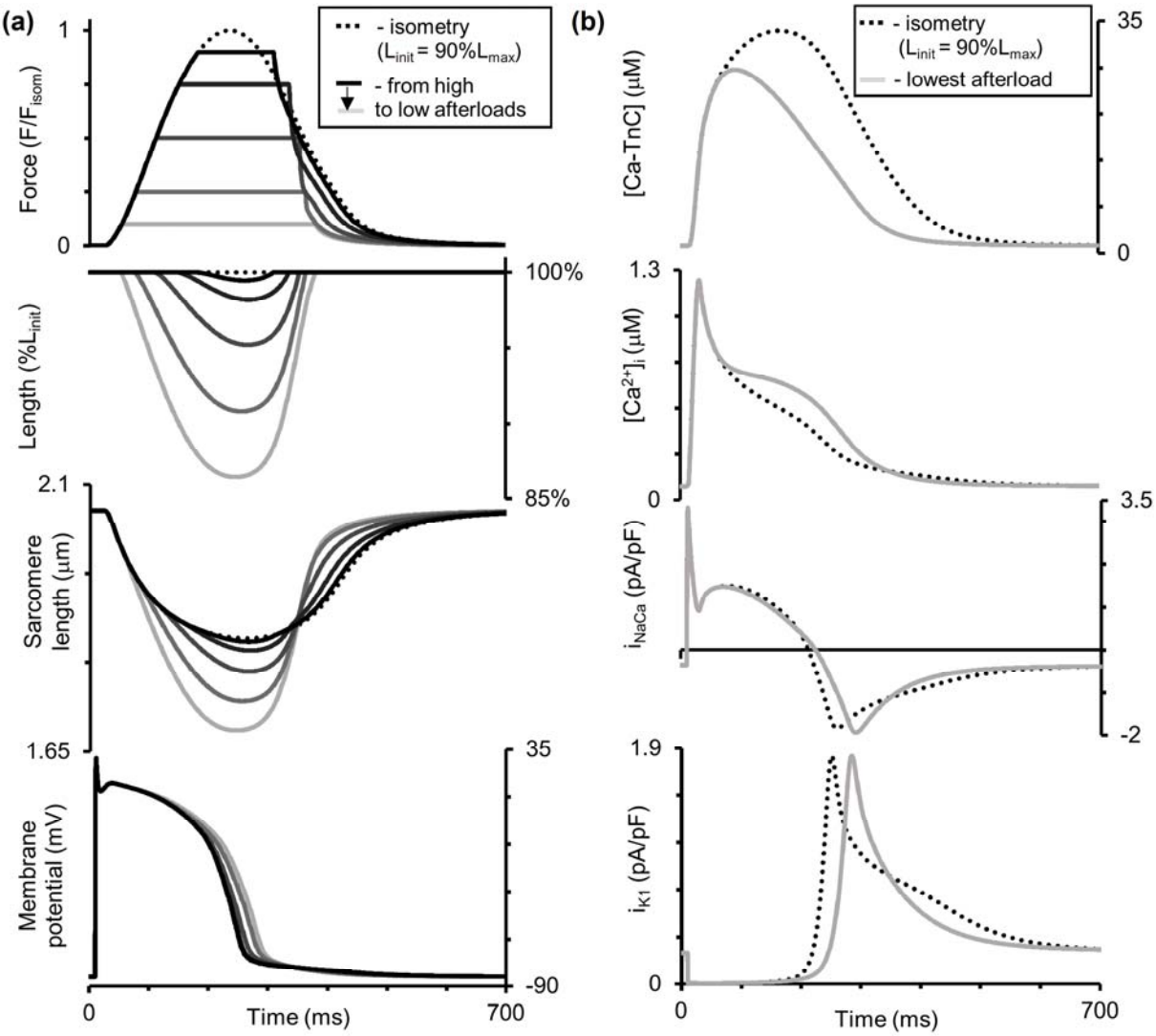

Fig. 3 Simulation of a series of isotonic contractions in the TP+M model. The initial virtual sample length L_{init} is equal to 90%L_{max}. F_{isom} is the peak isometric force at L_{init}. Each afterload was applied next to the steady-state isometric contraction (dotted lines) varying from a high afterload of 0.9F_{isom} (black lines) to a low afterload of 0.1F_{isom} (light grey lines). (A) Time-dependent signals of the generated force (F/F_{isom}), sample length, sarcomere length and membrane potential for various loads applied. (B) Time-dependent signals of the concentration of calcium-troponin C complexes ($[Ca\text{-}TnC]$), intracellular Ca^{2+} transient ($[Ca^{2+}]_i$), Na^+-Ca^{2+} exchange current (i_{NaCa}) and inward rectifier K^+ current (i_{K1}) for isometric and afterloaded contractions at the low afterload

Figure 3 shows results of our simulations using TP+M model for a steady state isometric contraction of a sample initially stretched by a preload to a length of 90%L_{max} (where L_{max} corresponds to a sarcomere length equal to 2.23 µm). Both time to peak isometric force and isometric relaxation time obtained in our simulations fit well into the range of the respective data obtained on papillary muscles, trabeculae and subepicardial biopsy strips from the human ventricles [45, 49, 52, 56, 62, 63]. The isometric signals are superimposed with ones recorded in simulated series of isotonic contractions under various afterloads, at the same initial length of 90% L_{max}.

Figure 3 demonstrates the load dependent relaxation in the TP+M model, i.e. an increase in the velocity of muscle lengthening (isotonic relaxation) with a decrease in the applied load (see the length panel in Fig. 3). As a result, the smaller the afterload, the greater the difference between the durations of the isotonic phase of shortening-lengthening and that of the phase of isometric twitch during which the generated force is higher than applied afterload. The isometric and isotonic forces shown in Fig. 3a reveal these differences. To quantify this difference, the load dependence index (LDI) is calculated at any certain level of afterload F_{isot} as the ratio of the time intervals shown in Fig. 4: LDI = t_{isot}/t_{isom} [59].

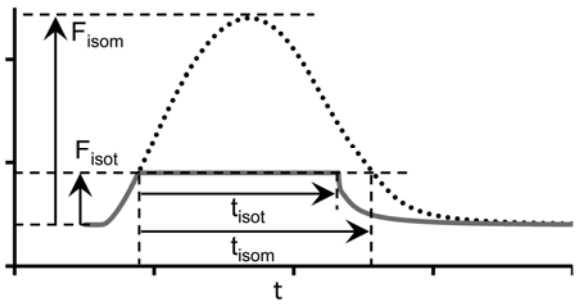

Fig. 4 The load dependence index (*LDI*) is set as ratio of t_{isot}/t_{isom}

Figure 5a shows the dependence of LDI on the normalized afterload F_{isot}/F_{isom} at two initial lengths (90%L_{max} and 95%L_{max}) in the TP+M model. It can be seen, that for both initial lengths LDI is less than 1 at low afterloads reflecting effects of muscle inactivation by shortening. This model prediction for the human myocardium fits well with the data obtain on various species, e.g. guinea pigs [59] and rats [64]. Unexpectedly, the LDI curve is independent of the initial sample length (preload) of the virtual sample.

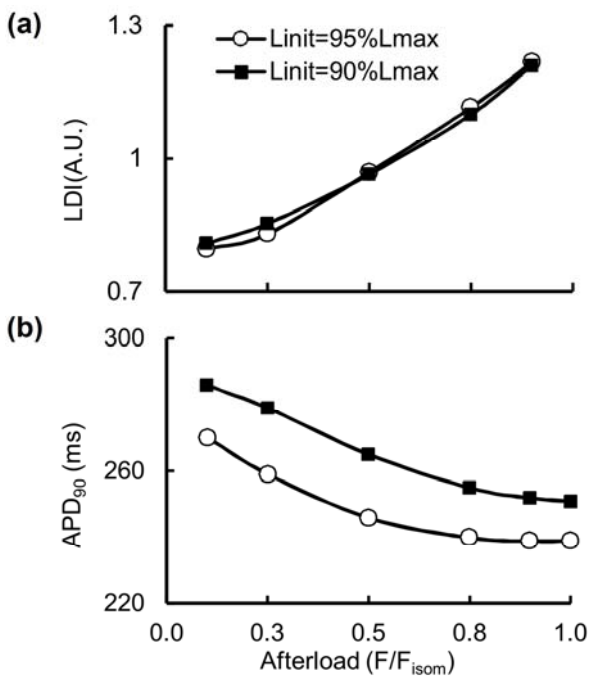

Fig. 5 Load dependent characteristics in the TP+M model for two initial virtual sample lengths L_{init}: 90% and 95%L_{max}. The abscissa axis shows the force values normalized to the maximum isometric value F_{isom} corresponding the initial length L_{init}. **a** The load dependence index *(LDI)* calculated as shown in Fig. 4. **b** Action potential duration calculated at the level of 90% of repolarization (APD_{90})

Figure 3b shows calcium transients ($[Ca^{2+}]_i$) in the virtual muscle cell during isometric (dashed) and isotonic (solid) contraction at the low load. The intermediate traces for Ca^{2+} transients are between these curves and not shown for the simplicity. Such load dependent elevation ("bump") in the decay phase of Ca^{2+} transient was shown in the myocardial preparations of various laboratory animals, e.g. rat, cat, rabbit [58]. This MCF effect arises in the TP+M model due to the increasing of the Ca-TnC complexes' dissociation (*[Ca-TnC]*, Fig. 3b) at faster and higher shortening under the low load (see the sample and sarcomere length changes in Fig. 3b) which occurs as a result of the length dependent cooperativity mechanisms in myofilaments.

This MCF, in turn, induces the MEF manifestations in the model shown in Fig. 3a: the smaller the load, the slower the repolarization phase and duration of the AP. Similar load dependent increase in AP duration (APD) was shown in cardiac preparations from various animals [58].

Note, that the combined model with the baseline TP parameters of Ca^{2+} currents did not produce such AP response to shortening, showing almost no effect of mechanical load on the AP. In order to simulate load dependence of AP in the TP+M model, we performed additional tuning of the parameters for the NCX current (i_{NaCa}, Fig. 3b). This current was shown to trigger AP modulations in response to load dependent modulations in the cytosolic Ca^{2+} concentration in the

‘Ekaterinburg – Oxford’ model [9]. Analysis of the TP+M model showed that the NCX is able to "transfer" a larger cytosolic Ca^{2+} concentration into a slowing repolarization at the low load, only if the reverse mode NCX current essentially contributes to the repolarization process. During the reverse mode, one Ca^{2+} ion comes from the extracellular space into the cytosol in exchange for three Na^{+} ions coming outside the cell. The higher the cytosolic Ca^{2+} concentration (i.e. the smaller transmembrane Ca^{2+} gradient), the smaller is NCX current during the reverse mode. In the original TP model, this NCX phase during the AP plateau was absent. To make the model produce the reverse mode NCX current, we changed the value of only one parameter in the NCX equation (4). This parameter α (see Supplement for NCX current description) controls the ratio between the positive and negative terms in the NCX formulation and thus allows one to get a positive outward NCX current during AP plateau, which contributes to AP repolarization.

Note that our assumption on the existence of the reverse NCX current during the cardiac cycle is speculative, but similarly speculative as the opposite assumption on its absence made in the original TP model. Because there is no direct experimental data on NCX time course in human cardiomyocytes, both assumptions can only be justified by speculations on the physiological feasibility of the reverse mode for the cellular outputs. In terms of AP generation, the outward NCX current during the AP plateau phase counteracts with the inward L-type Ca^{2+} current and thus does not support the plateau maintenance (e.g. see paper [65]). In ionic models focused only on the AP description, this reason can possibly be used to exclude the reverse mode NCX current without the loss of accuracy in simulated AP. However in terms of contraction, which is the main function of cardiomyocytes, the reverse NCX current brings Ca^{2+} into the cell, thus co-acting in the same direction with the L-type Ca^{2+} current and allowing more Ca^{2+} to support myofilament activation and further contraction. Importantly that the latter considerations were formulated in the experimental work dealing with the reverse NCX current in the human ventricular myocytes [66].

Being based on both the arguments by Weisser-Thomas et al. and on the important role of the reverse NCX current for the MEF proper for cardiomyocytes in most mammals we assume that the reverse mode NCX is present.

As a result NCX works as follows: under the low mechanical load due to bump of the Ca^{2+} the NCX current slightly decreases compared to the isometric conditions and as NCX acts in the reverse mode (i_{NaCa}, Fig. 3b) it slightly decreases repolarizing (outwards) current. Despite an apparently small effect, this triggers an initial slowdown in the repolarization of the AP in low mechanical load conditions compared to the isometry. It initiates a delay in the activation of the potassium currents (see Fig. 3b for i_{Kl}), which then causes prolongation of APD during isotonic contraction as compared to the isometric twitch. The prolongation is up to 14% and up to 13% compared to the isometric conditions for 90%L_{init} and 95%L_{init} respectively.

Figure 5b shows the dependence of APD_{90} on the relative afterload for isotonic twitches at two initial lengths of the virtual sample: 90%L_{max} and 95%L_{max}. It can be seen that at each initial length APD_{90} decreases with the increase in afterload. We see that APD_{90} also significantly depends on the initial length: APD_{90} for 90%L_{max} is located significantly higher than for 95%L_{max}. In contrast, the “Afterload – LDI” does not depend on the initial length (Fig. 5a). This significant distinction between the “Afterload – APD_{90}” curves for different preloads (initial lengths) is a model prediction, and as far as we know such effect was not yet studied in experiment for both human and animal myocardium.

3.1.2 Simulation of the physiological mode of contraction-relaxation cycles

A physiological mode of muscle contraction is used in experiments on heart muscle preparations (papillary muscles and trabeculae, [5]) to simulate the ventricular contraction phases during cardiac cycle: isovolumetric contraction, ejection, isovolumetric relaxation, and final filling. Plot of the ventricular volume against the pressure developed during the cycle (the “Pressure – Volume” (PV) loop) is conventionally used to characterize cardiac contractility [67]. The area of the PV-loop allow one to estimate mechanical work and power produced by the ventricle during the cycle [67].

In the physiological mode of contraction, a heart muscle preparation placed in the experimental setup consequently goes through the following phases of the contractile cycle (Fig. 6a,b): isometric contraction at a fixed initial length until muscle force approaches an imposed afterload level (reflects the phase of isovolumetric ventricular contraction); isotonic shortening down to an end-systolic length (ejection); isometric relaxation at the fixed end-systolic length (volumetric relaxation); and final stretch back to the initial length (filling). Similarly to the PV-loop, the “Length – Force” (LF) loop during the physiological contraction cycle is also used to evaluate muscle contractility, and the area of the LF-loop is used to calculate work and power of the muscle [68-70].

Note that physiological twitch differs from isotonic one only during the relaxation phase, i.e. after reaching the end-systolic length. Relaxation in the isotonic mode occurs under the same load with which the preparation shortened during the preceding contraction phase. In other words, in this case the preparation is stretched by the load during the relaxation phase until it returns to its initial (end-diastolic) length, at which the relaxation finishes isometrically. Unlike, in the physiological mode right after reaching the end-systolic length, the preparation starts to relax isometrically at this length, until its force

drops to the level of the initial preload. After that, the servomotor of the setup returns the preparation to the initial end-diastolic length with a constant velocity. The last stage is simulated in the model respectively as a stretching of the virtual sample with a prescribed velocity (see Supplement for length change description).

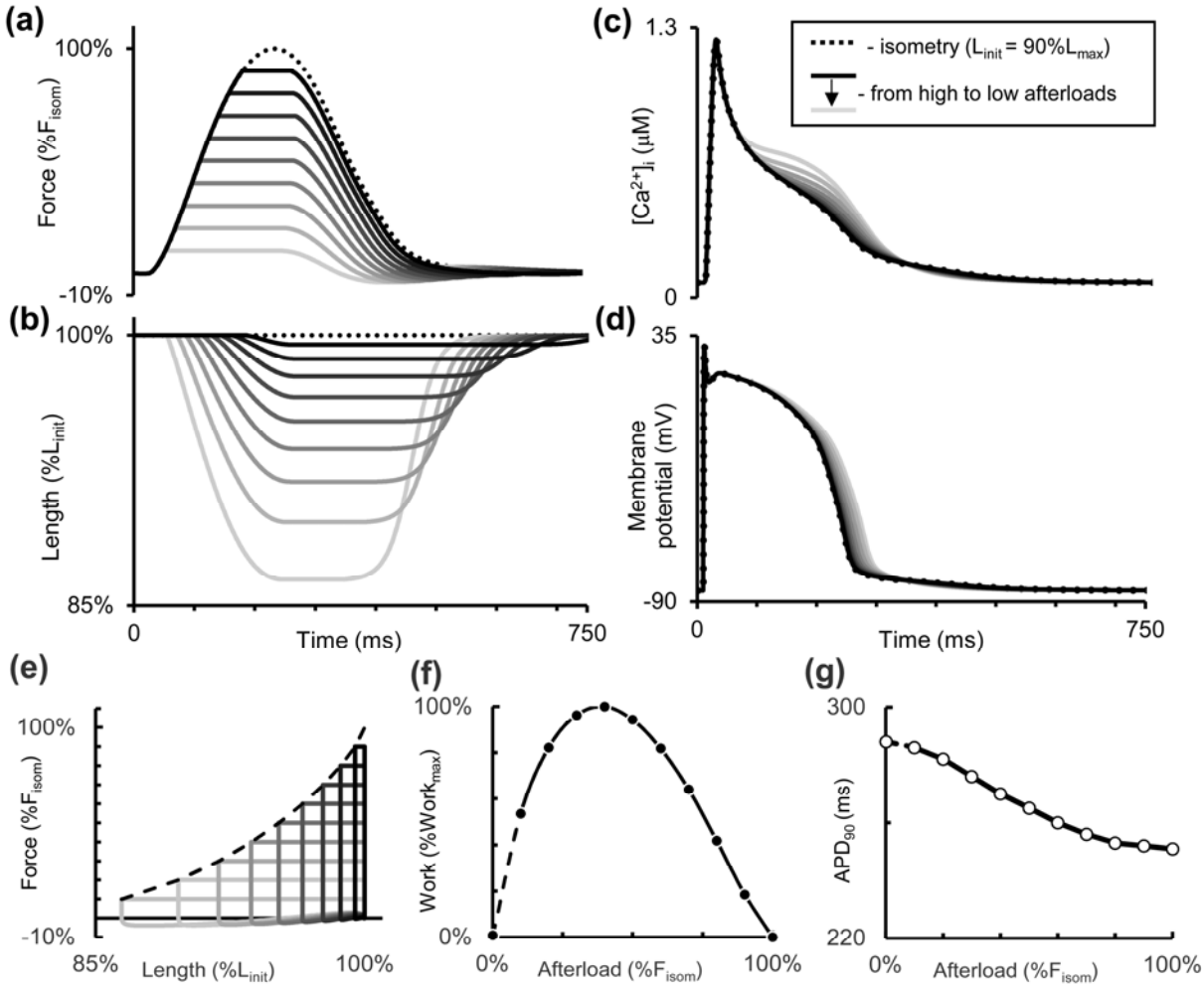

Fig. 6 Simulation of electromechanical activity of a virtual sample under a physiological sequence of loads (see text for details) in the TP+M model. The initial sample length L_{init} is equal to 90%L_{max}. In series of experiments the preload was applied right after the steady-state isometric contraction (dotted lines) changing from the highest afterload 90%F_{isom} (black lines) to the lowest afterload 0.1%F_{isom} (light grey lines), where F_{isom} is the peak isometric force for L_{init}. **a-d** Time course of force development, sample length changes, intracellular Ca^{2+} transient ($[Ca^{2+}]_i$) and membrane potential. **e** " Length – Force" loop-style curves for contractions under physiological sequence of load (solid lines). The dashed line connecting the top left dots of loops produces the "Force – End-systolic length" relation. **f** "Work – Load" relationship normalized to the maximum work value ($Work_{max}$) seen under 40%F_{isom} afterload. **g** Changes of action potential duration calculated on the level of 90% of repolarization under different afterloads

Figure 6a-d shows simulation of a series of contraction-relaxation cycles in the physiological mode under different loads at the initial length of 90%L_{max} in the TP+M model. The model results show that both MCF and MEF can be clearly seen in human cardiomyocytes in the physiological mode, which is closer to the loading conditions of the cardiomyocyte in the ventricular wall. Note that the relationship "Afterload – APD" (Fig. 6g) coincides with the similar dependence shown in Fig. 5b obtained for isotonic cycles at the same length of 90%L_{max}. This result suggests that load dependence of the APD_{90} is entirely determined by the contraction phase, which is the same in the isotonic and physiological mode of contraction, while the APD_{90} value itself corresponds rather to the early relaxation phase of the physiological twitches. Thus is because the reverse mode NCX current, initiating the process of the AP slowing down in afterloaded twitches, arises just during the phase of contraction (see Fig. 3), while this phase entirely coincides in the isometric and isotonic mode for the same afterload.

Figure 6e shows LF-loops plotted for all physiological cycles presented in Fig. 6a,b. The dotted line of the envelope of LV-loops shows the relationship between the end-systolic length and the force. In other words, it is so-called isotonic

"Length – Force" relationship (the term "isotonic" is correct in this case as this relationship is obviously the same as for the isotonic curves shown in Fig. 3).

An area of each LF-loop is equal to the useful work performed by the virtual sample at a given afterload during the shortening. The dependence of the work on the afterload is shown in Fig. 6f. It is seen that the maximum value of the work is achieved at the afterload of approximately 40% of the peak isometric force F_{isom}. This simulation result is consistent with the data reported in the only published experimental study where contractions of the muscle preparation from the human left ventricle were tested in the physiological mode [47]. It was shown that the maximum work performed by the muscle was registered at the middle afterloads [47]. In particular, the "Load – Work" dependence for the initial length of 90%L_{max} (*ibidem*) had the maximum between 40% and 50% of F_{isom}.

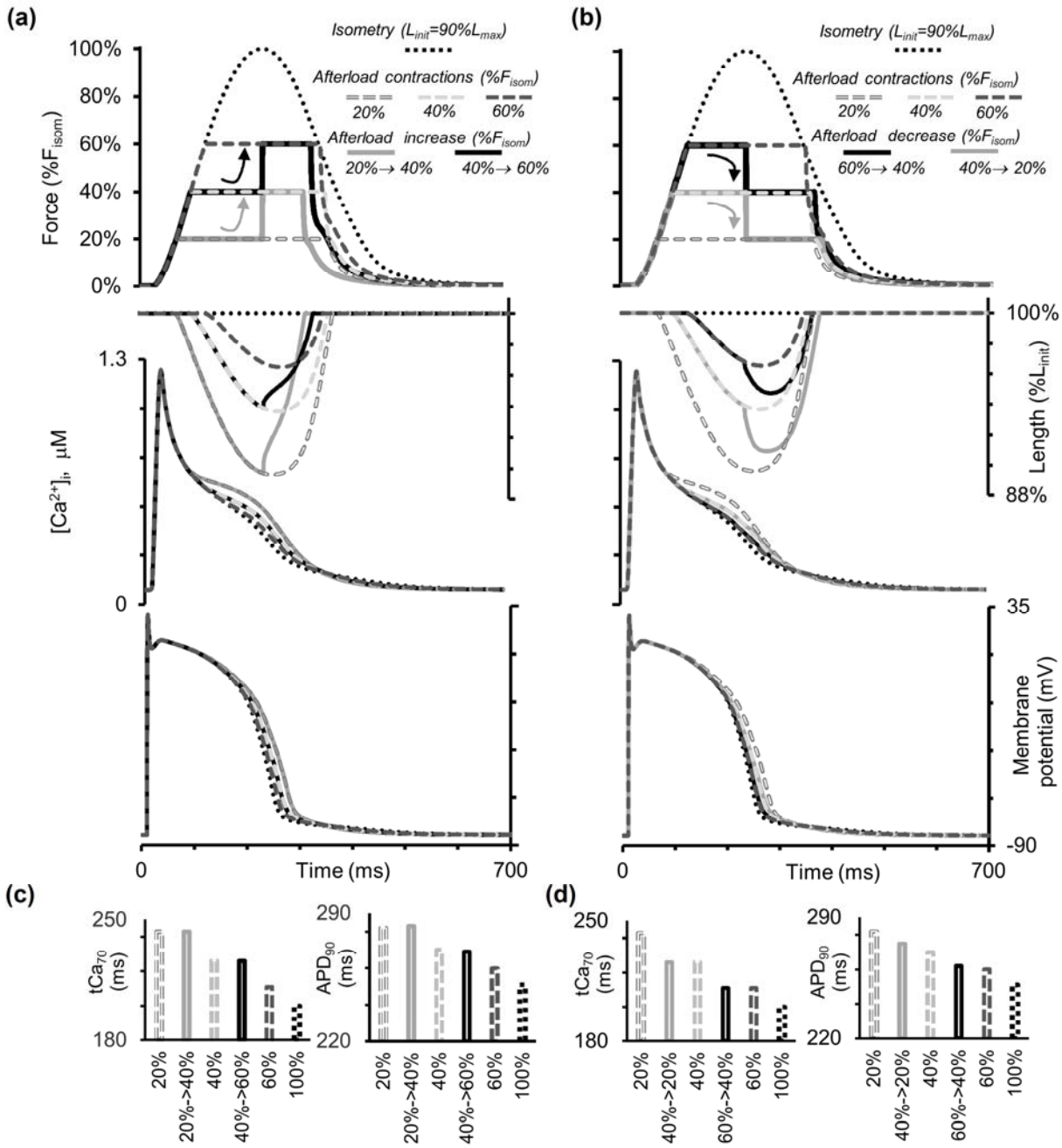

Fig. 7 Simulation of a quick change in the load during an isotonic cycle in the TP+M model. The initial virtual sample length L_{init} is equal to 90%L_{max}. Dotted lines are for isometric contraction. Dashed lines show afterloaded contractions under different loads (20, 40 and 60% of peak isometric force F_{isom} at L_{init}). Solid lines show the traces for quick increase **(a)** and decrease **(b)** in the load approximately at the middle of isotonic plateau. From top to bottom in both **(a)** and **(b)**: force, sample length, intracellular Ca^{2+} transient ($[Ca^{2+}]_i$) and membrane potential changes. **c-d** The value tCa_{70} is time from peak of Ca^{2+} transient to 70% decay. APD_{90} is action potential duration at 90% of repolarization

3.1.3 Simulation of modified isotonic twitches with quick load switches

Figure 7 shows the results of numerical experiments in which the load on the virtual sample was changed abruptly during isotonic contraction-relaxation cycles. The initial length was 90%L_{max} and the load was either increased (Fig. 7a) or decreased (Fig. 7b). In both cases, the load switching occurred approximately at the middle of the initial isotonic cycles, i.e. when the phase of isotonic shortening under the first load was almost finished. Such experiments were earlier performed on the guinea pig heart muscles [59], and on that of cats and rabbits [41], and mechanical responses to the load switches qualitatively similar to ones shown here (*Force*, *Length*, Fig. 7a-b).

Corresponding responses of the calcium transients ($[Ca^{2+}]_i$) and membrane potentials to the change in the applied load are shown in Fig. 7a-b. The diagrams in Fig. 7c-d show the values of APD_{90} and the duration of calcium transients (tCa_{70}) for all switches applied. It can be seen that despite large changes in mechanical conditions during the cycle, we do not observe significant changes in the characteristics of the APs and calcium transients, if we compare them to the values obtained in the usual isotonic twitches under the first load. This indicates that mechanical interventions imposed during the contraction phase affect Ca^{2+} kinetics and electrical activity more than interventions imposed during the relaxation phase.

3.1.4 Simulation of isotonic contractions phase followed by the quick muscle re-stretch to the initial length

The only experimental study demonstrating MCF in human cardiac muscle was study by [55] of modified isotonic twitches in the human trabeculae. We performed simulations in the TP+M model using similar protocol (Fig. 8). We see that both MCF (Fig. 8c) and MEF (Fig. 8d) manifest themselves here in the same manner as in all presented above afterloaded twitches.

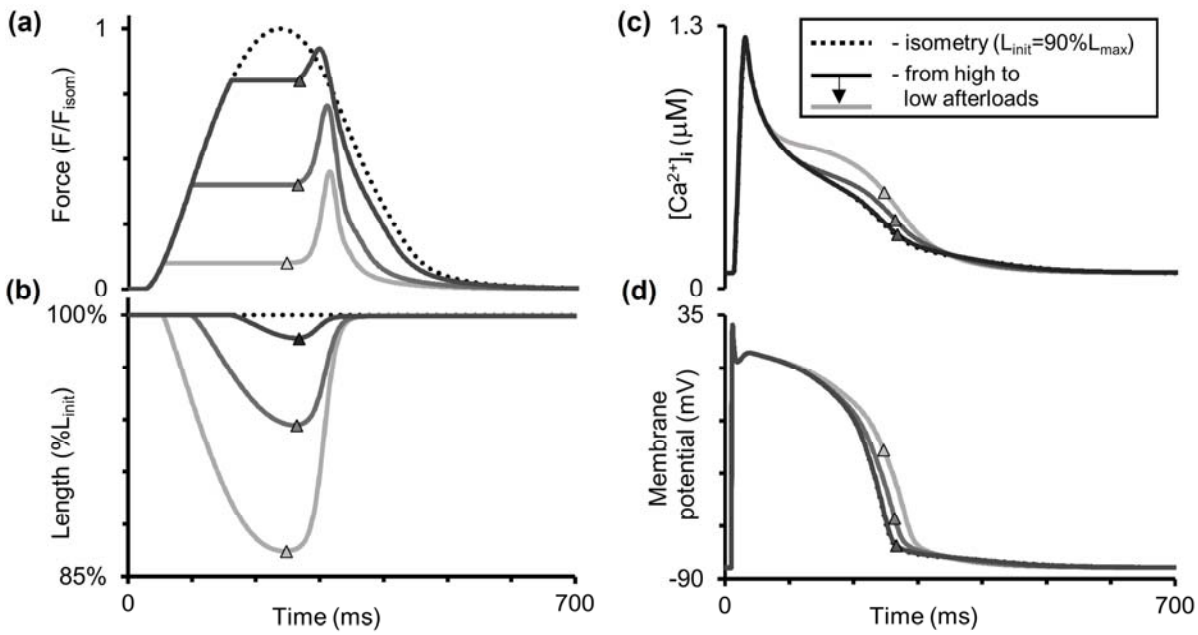

Fig. 8 Simulation of modified afterloaded contractions with quick muscle restretching in the TP+M model. The mode of the cardiac muscle contraction simulated in the following way. The muscle is allowed to contract against different loads (decreased in **(a)** from dark to light grey lines) in the same manner as in the isotonic mode. Then, at the moments of the maximum (end-systolic) shortening (shown by triangles) the muscle is forced to stretch with a velocity much higher than that of its lengthening in the full afterloaded cycle shown for the virtual sample in Fig. 3. Thus, the sample quickly returns to its initial length (L_{init} = 90%L_{max} in this simulation) and then relaxes isometrically. Dotted lines are for the isometric contraction. **a-b** Active force normalized to the peak isometric one at L_{init}; length of the virtual sample (in % of L_{init}). **c-d** Intracellular Ca^{2+} concentration ($[Ca^{2+}]_i$) and membrane potential

4 Simulation of the length effects on the mechanical and electrical characteristics of the steady state isometric twitch

Using TP+M model we also reproduced the experimentally recorded isometric twitches of isolated human trabeculae when the muscle length was reduced in a stepwise fashion [56]. This paper presented only mechanical records (length and force), whereas our simulations reveal (Fig. 9) mechanical and electrical signals and calcium transients obtained at various lengths (from 80%L_{max} to 95%L_{max}) under steady state conditions for the pacing rate of 1 Hz. As in Fig. 3, in Fig. 9b we

presented the curves only for extreme cases (for the largest and smallest lengths). Both MCF ($[Ca^{2+}]_i$, Fig. 9b) and MEF (membrane potential, Fig. 9a) can be clearly seen. Fig. 10c shows the negative dependence of APD_{90} on the length. The mechanisms of this dependency is the same as we discussed above for the case of isotonic twitches.

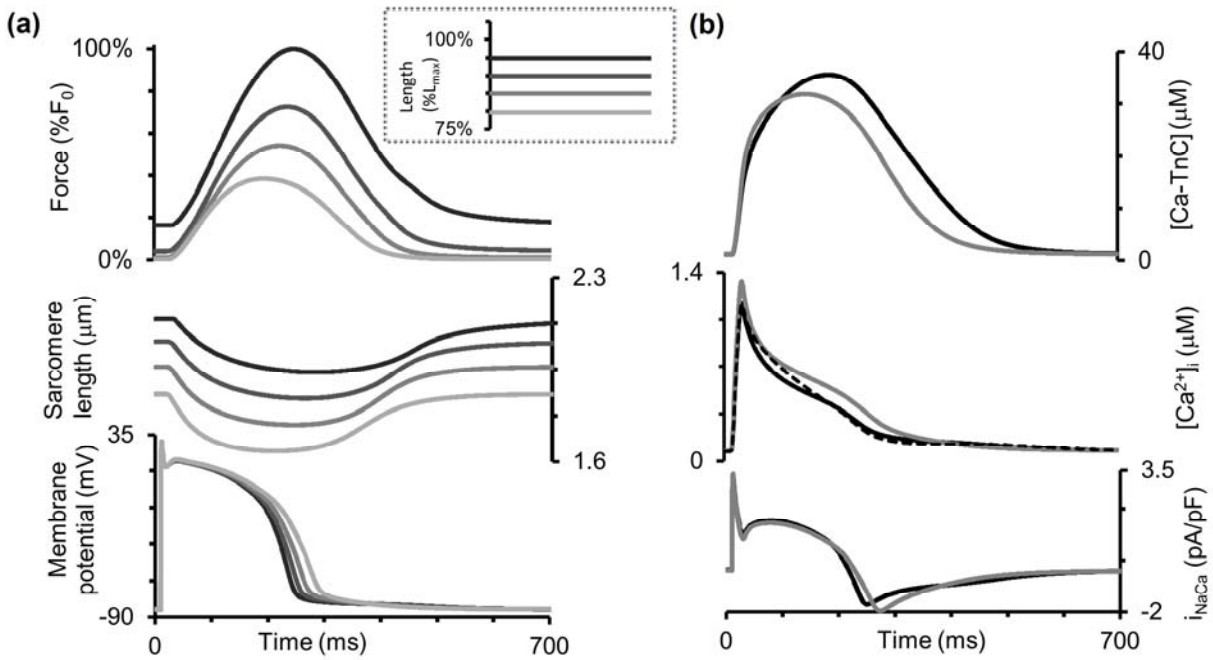

Fig. 9 Simulation of isometric contractions at different sample lengths in the TP+M model. The initial length of the sample was decreased from 95% to 80%L_{max} (see inset from dark to light grey lines). **a** The steady state signals for isometric force (as compared to the force F_0 generated at 95%L_{max} initial length), sarcomere length, and membrane potential are shown for all lengths considered. **b** The steady state signals for concentration of calcium-troponin C complexes ($[Ca\text{-}TnC]$), intracellular Ca^{2+} concentration ($[Ca^{2+}]_i$) and Na^+-Ca^{2+} exchange current (i_{NaCa}) for 85% and 95%L_{max} initial lengths. Dashed line in the intracellular Ca^{2+} concentration panel is for the numerical experiment where mechano-electric feedbacks were eliminated in the model by imposing isometric conditions on the sarcomere (see text for details)

Note, that AP durations for various lengths in Fig. 9 vary between 230 and 290 ms that corresponds to the experimental range of APDs recorded in human cardiomyocytes at 37°C with the pacing rate of 1 Hz, using the microelectrode technics [21] (see Fig. 6 of the cited article).

Temporal characteristics of Ca^{2+} transient, time to its peak included are in concordance with experimental data measured in a healthy isolated human ventricular myocyte at 37°C using Fura-2-AM and Fluoforte fluorescence data [21, 71]. Noteworthy, that there is a wide diversity of the experimental data on the time-to-peak $[Ca^{2+}]_i$ in humans. This might be due to differences in the dyes used, temperatures, and mechanical conditions in which myocardial preparations were tested. Anyway, it would be impossible to fit up the model to all these diverse data simultaneously.

As stated above both time to peak isometric force and isometric relaxation time obtained in our simulations fit well into the range of the respective data obtained on papillary muscles, trabeculae and subepicardial biopsy strips from the human ventricles [45, 49, 52, 56, 62, 63].

Similarly to the experiments under isometric conditions, our model in case of fixed sample length accounts for changes in sarcomere length due to in-series elastic compliance at the preparation boundaries (see Fig. 2). Note, that the decay of Ca^{2+} transient at the fixed sample length has two phases of changing convexity from positive to negative values, which manifests itself as a bump. We related this biphasic Ca^{2+} decay to the change in the sarcomere length during the isometric twitch of the sample. To check this hypothesis we eliminated effects of sarcomere shortening in special numerical experiment by fixing the contractile element representing sarcomeres in the model (see Fig. 2) at its initial length during entire contraction-relaxation cycle. As a result, the Ca^{2+} transient decay under isometric mode of the sarcomere contraction became monophasic (see the dashed line in the Ca^{2+} transient panel in Fig. 9) repeating respective feature of the Ca^{2+} transient in the original TP ionic model [20], in which mechanical factors are absent. Thus, the biphasic Ca^{2+} decay in TP+M model results from the MCF.

Monophasic Ca^{2+} transient decay was recorded in experiments in the human myocardium preparations with the eliminated mechanical activity (the tissue was immobilized by blebbistatin) [72], except the small islands of special cells (M-cells). On the other hand, biphasic Ca^{2+} transient was registered in trabeculae of the right ventricles of the guinea pigs

and rats contracted isometrically where internal sarcomere shortening was allowed [73]. Thus, our simulations of the Ca^{2+} transient decay in the TP+M model are consistent with these experimental studies and show that biphasic decay is a result of MCF in the cardiomyocytes.

Figure 10 presents inotropic and lusitropic length dependent characteristics for the simulated isometric twitches, in particular, isometric "Length – Force" relationship (Fig. 10a) that is commonly considered as an equivalent of the Frank-Starling's heart law for isolated myocardial preparations. The plot shows the peak isometric force against respective length of the virtual sample. The peak force increases with the length.

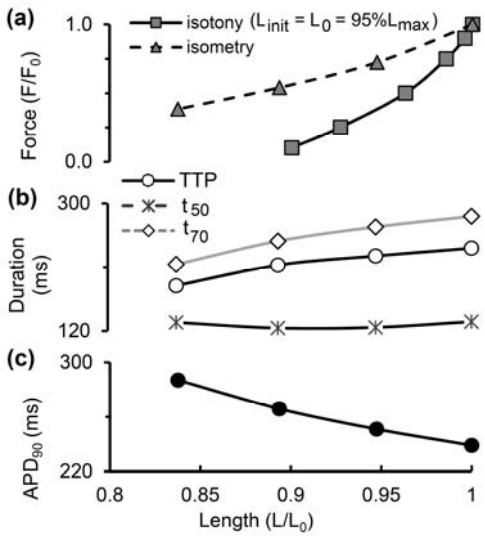

Fig. 10 Main characteristics of the isometric cycles in the TP+M model. **a** Solid line is for "Length – Force" diagram depicting relationship between end-systolic shortening and end-systolic force obtained in series of afterloaded contractions at initial length L_{init} = 95%L_{max}. Dashed line is for "Length – Force" diagrams depicting relationship between length and generated force obtained in series of isometric contractions, where length decreases from a reference length $L_0 = L_{init}$ (at which a virtual sample generates maximum isometric force F_0) to 84%L_0. **b** Length dependence of temporal characteristics of isometric twitch: *TTP* – time to peak of twitch; t_{50}, t_{70} – time to 50% and 70% force decay from peak force in isometric cycles. **c** Length dependence of action potential duration at 90% of repolarization (APD_{90}) in isometric cycles

In the fifties of the last century, the slope of the isometric "Length – Force" curve was attributed solely to the change with length of the overlap zone of thick and thin filaments. However, with more careful measurements it became clear that this slope is steeper than that which would occur only from the changes in the overlap zone. Later, it became generally accepted that, in addition to the overlap zone, calcium inactivation of the contraction during the sarcomere shortening (i.e. MCF) contributes to the slope of the isometric curve. For the comparison, Fig. 10a shows an isotonic "Length – Force" curve (solid line) for an initial length of 95%L_{max}, repeating the data shown in Fig. 6e. The steeper slope of this curve is known from numerous experiments on animals [41]. The TP+M model predicts the same for the human myocardium. The steeper slope of the isotonic curve is due to the higher sarcomere shortening velocity in isotony compared to the isometry, since the kinetics of attachment/detachment of the cross-bridges in the model is regulated not only by the length, but also by the velocities of the sarcomere shortening/lengthening. The increase in velocity affects a decrease in the number of the attached cross-bridges (via the mechanisms of cooperativity) and thus facilitates inactivation of Ca-TnC complexes.

Figure 10b shows time characteristics of the isometric contraction and relaxation for different lengths, namely: the time to the peak force (*TTP*) and the relaxation time, which is estimated by two indices (t_{50} and t_{70}). t_{50} is the time interval from the moment of the peak of contraction (i.e., from *TTP*) to the decline in the active force by 50% during the relaxation phase; while the t_{70} – by 70%. The mechanics of isometric cycles of contraction-relaxation of the human myocardium, unlike that of isotonic ones, was studied in large number of experimental papers [42-57]. Not all of them had systematically studied the length effect on inotropic and lusitropic characteristics of the human myocardium. Nevertheless, they provide the experimentally observed ranges of TTP, t_{70} and t_{50} values which we used for verification of the parameters of the TP+M model responsible for its mechanical behavior. Thus, our simulations are within the ranges of these mechanical characteristics obtained in the referenced above experiments.

The upper panel in Fig. 9a allows us to correlate the length dependent decrease in contraction and relaxation times revealed in Fig. 10b with the calcium inactivation of the cardiomyocyte, i.e. with the more intensive decay of the Ca-TnC complexes at shorter lengths.

5 Simulation of mechano-calcium and mechano-electric feedbacks in response to the quick release of the human myocardium at different moments of isometric twitch

Figure 11 shows the results of the instantaneous release of the virtual sample initially contracting isometrically at the length of 90%L_{max}. The sample is shorten quickly by 5% of the initial length at different moments of the isometric twitch (Fig. 11a), and then contracts/relaxes in isometric mode at this smaller length (Fig. 11b). Similar experiments were performed on the papillary muscles of various animals, for example, cats and ferrets [58].

Mechanical inactivation manifests itself as a decrease in the developed force of the virtual sample, which is accompanied by increase of free cytosolic calcium upon the decay phase of Ca^{2+} transient (Fig. 11c) and by the AP prolongation (Fig. 11d). Additional free cytosolic Ca^{2+} occurs after the quick release due to the additional Ca-TnC dissociation caused by the mechanical perturbation. As in simulations presented in Fig. 3, here, we also observe APD prolongation (Fig. 11). However, the mechanism of this effect is different. In Fig. 3 the prolongation was a result of reduced repolarization current produced by NCX in the reverse mode. In the case of the later length release in Fig. 11, the reverse NCX current has already became forward depolarizing current. Therefore, the mechano-dependent increase in free cytosolic Ca^{2+} led in this case to the increase in this depolarizing NCX current and thus to the observed AP prolongation. Thus, the abrupt decrease in the length even during the relaxation stage resulted in the prolongation of both calcium transient and AP.

The TP+M model also provides data on the dependence of Ca^{2+} transient and AP time course on the amplitude of quick releases (not shown).

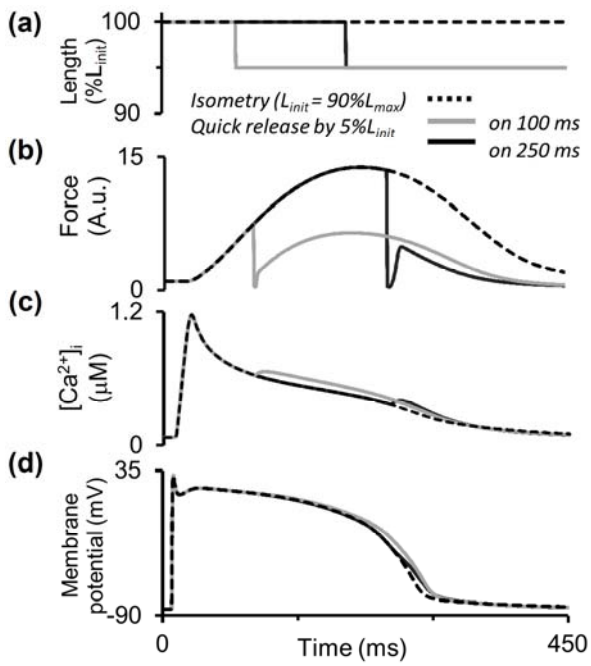

Fig. 11 Simulation of quick releases of a virtual sample during isometric cycle in the TP+M model. The initial length L_{init} is equal to 90%L_{max}. The sample is quickly released to 95%L_{init} at 90 and 240 ms after the stimulus and is held at a new length until the end of the cycle. **a-d** Length of virtual sample, force development, intracellular Ca^{2+} transient ($[Ca^{2+}]_i$) and membrane potential in the simulation

6 Discussion

MEF and MCF are an important way of the adaptation of cardiomyocytes to the mechanical conditions of their contraction in the walls of the heart chambers, including adaptation to the conditions of the mechanical interaction between heterogeneous cardiomyocytes. Elucidation of the mechanisms underlying MEF and MCF is one of the most complicated physiological problems. A number of studies including experimental works and modeling are aimed to shed a light on this subject [1-3, 9, 24, 74-76]. The effects of MEF and MCF can be separated into two large groups: fast and slow responses of a cardiomyocyte to mechanical influence. Each of these two groups requires a separate study, since there are serious reasons to believe that the mechanisms underlying them may not coincide.

In particular, it is commonly recognized that contribution of such direct MEF sources as stretch-activated channels (SACs) is very important factor of the slow responses. However, to explain the fast responses that occur during one cycle of contraction-relaxation, other more complex multi-step mechanisms are to be involved.

To study fast responses of the human cardiomyocyte to the mechanical impacts we have developed the TP+M model of the electromechanical coupling in the human cardiomyocytes based on the 'ten Tusscher – Panfilov' electrophysiological model and the module of the mechanical activity taken from the 'Ekaterinburg – Oxford' model. We implemented the main experimental modes of the cardiac muscle contraction-relaxation cycles (isometric, isotonic and physiological ones) to the TP+M model, and studied the effects of mechanical conditions on the contractile cycle.

In the TP+M model, we investigated fast responses of the virtual heart muscle to the mechanical modes, namely:

- responses to the load, under which the sample contracts in the isotonic mode, and in various modifications of this mode (Fig. 3, 6, 7, 8);
- responses to the fast shortening of the sample at different moments within the contraction-relaxation cycle (Fig. 11).

The quick release of the heart muscle to its shorter length (Fig. 11) lasting only a few milliseconds reduces mechanical activity of the cardiomyocytes throughout the whole current contraction-relaxation cycle much more significantly than a simple reduction of the thin and thick filament overlap zone in the sarcomeres might provide. A little further, we discuss the reasons of the irrelevancy of the SACs to be involved as explanation of this effect.

The only fragment of our presented study where we deviated to some extent from the subject of fast responses was simulation of isometric contractions with various initial lengths (pre-stretching) of the virtual sample. The reason was that we used the results of these simulations to verify the model by comparing these results with the corresponding data from physiological experiments [56]. These physiological data were obtained in series of steady state isometric contractions with fixed pacing rate of 1 Hz at different lengths of each tested muscle preparation. Accordingly, the model was assigned to be in the same conditions. Thus, the characteristics of isometric contractions shown in Fig. 9 and Fig. 10 were obtained at different lengths just when simulating series of steady state isometric contractions at the frequency of 1 Hz. These characteristics really fall into the ranges of values reported both in the cited work [56] and in other experimental works where the data obtained in isometric contractions of the human myocardium at one or another length were provided, although the effect of the differences in the length was not specially studied [45, 51, 52, 63].

According to the TP+M model, mechanical conditions should have an effect on the duration of both action potential and calcium transients in the human cardiomyocyte and contribute substantially to their mechanical activity. For instance, the smaller afterload in isotonic cycles, the longer AP and Ca^{2+} transient duration, while the shorter duration of the mechanical twitch (Fig. 3). These results are predictions of the TP+M model, which cannot be directly experimentally confirmed or rejected today due to the absence of the respective experimental data that would be obtained on the human myocardium. Nonetheless, these results of the modeling seem to be reasonable, since similar manifestations of the MEF and MCF have also been found in numerous experiments on animals.

Really a large number of classical experimental studies on preparations of the heart muscle [58, 77, 78] and theoretical work using mathematical models [9, 24, 79, 80] has been aimed to the search of the mechanisms determining just the fast myocardium adjustment to changes in the mechanical conditions of its contraction, in particular, to the fast decrease in its length or the applied load. Max Lab has shown in his experiments that additional free calcium occurs in the cytosol in response to a decrease in length or load, and this surplus of the calcium transient is partially retained during most of the subsequent phase of the contraction-relaxation cycle, even if the mechanical impact has already disappeared (for example, if, after a quick release, the preparation has been then quickly returned to its initial length) [58]. In the same experiments, it was found that along with this modulation of the calcium transient, the AP duration increased, while the ability of the muscle to develop active force decreased, and this mechanical inactivation continued until the very end of the contraction-relaxation cycle.

As mentioned above, these load and length dependent events cannot be explained by SACs, because, firstly, additional free calcium arose in response to shortening, but not to stretch, and secondly, if this additional Ca^{2+} initiated by the mechanical impact entered the cell from the outside, then it would rather additionally activate the cell, while the inactivation was observed in the reality. The following mechanism was suggested in many of the cited works to explain all of these events at once. When the sarcomere shortens, the dissociation of Ca-TnC complexes increases, which simultaneously causes both observed events: the inactivation and an increment of the free Ca^{2+} concentration. In turn, this additional free cytosolic Ca^{2+} increases the AP duration by means of the NCX current.

In this hypothetical chain of intracellular mechanisms, the most difficult to explain was the assumption of the increased dissociation of Ca-TnC complexes in response to the myocyte shortening. We first suggested possible explanation of this increase and justified it in the framework of mathematical modeling in 1991 [41]. The main link of the concept proposed in that our work was one of the known mechanisms of cooperative interaction of regulatory and contractile proteins: the lower concentration of the cross-bridges attached to the thin filaments near a Ca-TnC complex, the more probable dissociation of this complex [13, 81, 82]. Combined with a decrease in the probability of the cross-bridge attachment during the sarcomere shortening, this cooperativity provided the key to understanding the length dependent

decrease in the Ca-TnC decay. Particular mechanisms underlying the length effect on the cross-bridge attachment are being debated [35, 38, 83, 84]. During a long time the most accepted explanation of this effect was lattice spacing concept that fitted sarcomere interfilamentous distance and thus probability of the cross-bridge attachment to the sarcomere instant length [35]. However, recent experimental works allow their authors to suggest that the giant protein titin rather than the lattice spacing effects determines the length dependence of the cross-bridge attachment [38]. It was also supposed that lattice spacing modulation does exist, but it is just titin-based [84]. Anyway, the length dependence as such is an invariant of the underlying it mechanisms and is accepted by all authors.

Incorporation of these mechanisms in the model of mechanical activity of the myocardium [41], and then in the 'Ekaterinburg – Oxford' model of the electromechanical coupling in the myocardium of guinea pig and rabbit [9] has allowed us earlier to reproduce and explain practically the whole range of phenomena associated with fast responses to mechanical impacts within the framework of those models.

Later, other authors also used similar approaches in the models they develop, for example, in Landsberg and Sideman model [85], Jeremy Rice model [26], Lauren Dupuis model [86, 87], in which contribution of mechanical conditions of the contractions to the myocardial mechanical activity was studied and applied to assess and analyze *in vitro* data obtained in experiments on various warm-blooded animal heart muscles. The contribution of length and/or load to the Ca-TnC kinetics is justified differently in these models and is consequently given by different formulas in the equations describing this kinetics.

For example, in the Dupuis model, like in ours, the source of the mechano-dependent kinetics of Ca-TnC is the cooperative effect of the cross-bridges on the affinity of Ca-TnC complexes. Moreover, the authors of the cited model very carefully substantiate the formulas that determine the contribution of this cooperativity. As a result, their model adequately reproduces both load dependence of isotonic twitches and length dependence of isometric twitches. The calcium transient in the original Dupuis model is defined simplistically as an explicit function of time; therefore, the problem of MCF and MEF cannot be investigated directly within this model framework. To solve this problem, the Dupuis model should be combined with one or another model of intracellular Ca^{2+} handling and AP generation, and the result will obviously depend on the properties of all combined components.

In the Rice model, the contribution of the length to the Ca-TnC kinetics is given by rather arbitrary simplified formula, and this model reproduces successfully the length dependence of the isometric twitches (including the influence of the preloads, i.e., of the lengths on the Ca^{2+} transients in these twitches), but not the load dependence of the isotonic twitches.

Despite the repeatedly confirmed presence of the fast effects of MEF and MCF in the myocardium of various animals (rat, cat, rabbit, dog, guinea pig, etc.), it still remains unclear whether these effects are characteristic for the human myocardium, and even if they are, the same or not the same mechanisms underlie these effects in human. Very limited amount of experimental data has not allowed of getting a clear answer to these questions in the framework of experimental physiological studies as yet. In such a situation, the use of mathematical modeling as a tool for at least initial predicting of the possible answers becomes greatly needed. Noteworthy that the answers to the stated questions in the framework of the modeling approach was a priori far from obvious. For instance, a recent attempt to assess the MEF effects in the framework of the electromechanical model formed by coupling the Rice mechanical model with the electric models of cardiomyocytes of various animals led the authors of the cited article to conclude that MEF effects occur in the dog's myocardium, however practically absent in that of human [24]. Of course, the result they obtained significantly depended on the properties of the coupled models, including the features of the Rice model that we just mentioned. Therefore, their conclusion seems quite debatable, especially taking into account the presence of such feedbacks in all other studied mammals.

In this work, we did not deal with slow force responses such as experimentally shown transient process that occurs during a series of contractions after a rapid increase in the length obtained, for example, in experiments on rat and cat myocardium preparations [76, 88]. The essence of the referred slow force response is as follows. When a muscle preparation is stretched from a shorter length to a larger one an increase in the peak isometric force occurs not only in the first contraction immediately following this muscle stretch. Not very big, but quite noticeable further increase in the force amplitudes proceeds beat-to-beat in a series of subsequent isometric contractions with a fixed stimulation frequency during a relatively long transient process. Along with the force, $[Ca^{2+}]_i$ peak also gradually increases beat-to-beat during this process.

These slow responses of force and calcium seem impossible to explain by means of the length dependent kinetics of Ca-TnC alone. Therefore, to reproduce and explain it within the framework of any mathematical model, some additional intracellular mechanisms should be embedded in it. In particular, SACs may mediate Ca^{2+} entry during the slow response. It has been assumed, for example, that stretch induced increase in $[Ca^{2+}]_i$ during this transient process may occur either directly or indirectly by conducting Na^+ through the SACs, which in turn stimulates outward NCX current [89]. Not all researchers suggest that SACs are the main factor underlying the discussed slow response [76, 90]. It seems to be useful to

verify this hypothesis in the framework of mathematical modeling. However, we are convinced that for doing this in our model it would make sense to carry out a truly complex work, rather than simple fitting of the model to the desired result by including in it a hypothetical stretch-activated current as a nebulous entity which in any particular case would be transfigured and attributed to specific convenient properties a priori suitable for obtaining this result.

In such a complex study, it should be undoubtedly taken into account that "despite many experiments confirming the presence of mechanosensitive channels in cardiomyocytes [80, 91-93], there is a large variation in reports of both their characterization, and their effects on AP form and duration" [94]. Particularly, "APD has been shown both to increase [91, 95] and decrease [96] in response to the axial strain" [94]. According to the cited article, the most prevalent SACs are instantly-activating, non-inactivating, cation-selective ones conducting potassium and sodium currents. Referring to various experimental studies, the authors of this article emphasize that the reversal potentials of stretch-activated currents range from −75 to +10 mV [97], and conductance ranges from 10 to 200 pS [97]. Therefore, for example, even "the inward rectifier K^+ current has been observed both to increase [91] and decrease [98] in response to different mechanical stimuli" [94]. Thus, the contribution of various SACs to the AP development can occur both repolarizing and depolarizing, depending on the moment of the mechanical impact application, on its duration and magnitude, and, most importantly, on the magnitude of the reversal potential.

Under conditions of such great uncertainty and a variety of experimental data, SACs with initially undefined values of the parameter responsible for the reversal potentials and conductance of these channels can be incorporated in a model that has MCF and MEF loops based on the length dependent Ca-TnC kinetics, for trying to solve the inverse problem of the modeling for these parameters. The latter means to find such parameter values within the experimentally determined ranges that would permit to obtain simultaneously the whole complex of fast and slow responses of the heart muscle to the mechanical impacts. In other words, this means such values of the parameters for SACs, which would provide the slow responses without ruining the fast ones in the model.

Despite the inverse problem stated above has not been solved as yet, the introduction of SACs in various models is still possible and useful, but only to simulate relatively local situations pertaining to the stretch, since in these cases only arbitrarily values of reversal potentials and conductance (albeit within experimentally reported ranges) may be implemented. For example, it has been shown that SACs introduced in a model suchwise do simulate the slow response of the voltage and $[Ca^{2+}]_i$ to an increase in the length [75]. However, the fast responses, for example, such as load dependent relaxation and inactivation of the contractile cycle during quick deformations, were not simulated in this work.

Despite the undoubted local expediency of such approaches, they leave open the question concerning the complex role of SACs in the full spectrum of fast and slow responses. Therefore, even taking into account the fact that the inverse problem formulated above is very intractable, it seems nonetheless important to try solving it. Indeed, against the background of a huge scatter of experimental data, justified values of both reversal potentials and conductance for SACs, obtained in such integrative study of fast and slow responses within the framework of a mathematical model, would be useful for electrophysiology.

We emphasize that for a correct answer to the question stated and solved by us in this paper, whether the mechanisms of the length dependent cooperative influence of the cross-bridges' attachment on the Ca-TnC kinetics may provide as such both MEF and MCF related the fast responses of the human cardiomyocytes to the mechanical impacts, it was methodologically right to include in the model only these mechanisms. Of course, this does not mean that additional inclusion of SACs in the model will never make any sense when simulating the fast responses. On the contrary, if in the future we introduce these channels into the TP+M model and try to solve the formulated inverse problem, we will be able to evaluate whether they bring any modulations to the fast responses, and if so, which particular ones. On the other hand, maintaining the correct simulation of the fast responses after incorporating SACs into the model will be a strongly required condition and therefore a fundamental test for rejecting unacceptable hypothetical properties of these channels, initially inevitable due to the indicated above enormous uncertainty of these properties.

Conclusion

The TP+M model predicts that mechano-calcium, mechano-electric and mechano-mechanical feedbacks are to be inherent in the human cardiomyocytes. The key link underlying these feedbacks observed in the TP+M model during fast responses on the mechanical impacts is cooperativity of regulatory and contractile proteins. These feedbacks arise due to the following mechanisms implemented in the model: the shortening affects Ca-TnC kinetics and thus intracellular calcium kinetics, and through the NCX it results in the length/load dependence of the APD.

List of abbreviation

AP, APs	Action potential, action potentials
APD	Action potential duration
APD_{90}	Action potential duration calculated at the level of 90% of repolarization
Ca-TnC	Calcium- troponin C complexes
$[Ca^{2+}]_i$	Free cytosolic calcium concentration
ECC	Excitation-contraction coupling
F_{isom}	Peak isometric force
F_{isot}	Level of afterload
i_{NaCa}	Na^+-Ca^{2+} exchanger current
LDI	Load dependence index
LF-loop	"Length – Force" loop
L_{init}	Initial virtual sample length
L_{max}	Length corresponds to a sarcomere length equal to 2.23 μm
MCF	Mechano-calcium feedback
MEF	Mechano-electric feedback
NCX	Na^+-Ca^{2+} exchanger
PV-loop	"Pressure – Volume" loop
SACs	Stretch-activated channels
SR	Sarcoplasmic reticulum
SS	Subspace
tCa_{70}	Time from peak of Ca^{2+} transient to 70% decay.
TnC	Troponin C
TP model	'ten Tusscher – Panfilov' ionic model
TP+M model	Developed electromechanical model
TTP	Time to peak of twitch
t_{50}, t_{70}	Time to 50% and 70% force decay from peak force in isometric cycles
Xb, Xb-s	Cross-bridge, cross-bridges

Author contributions All authors contributed to conception and design of research, analyzed data, and interpreted the results of numerical experiments; NBV and LB developed the TP+M model; NBV performed numerical experiments; LB and NBV drafted the manuscript; all the authors edited, revised the manuscript, and approved the final manuscript.

Funding The work was carried out within the framework of the IIP UrB RAS themes (Nos. AAAA-A18-118020590031-8, AAAA-A18-118020590134-6) and was supported by RFBR (18-01-00059) and by Act 211 Government of the Russian Federation, contract No 02.A03.21.0006.

Acknowledgements Not applicable

Availability of data and materials The authors declare that all equations of the developed mathematical model, its parameters and initial values of phasic variables are available within the article and its supplementary information file.

Compliance with ethical standards

Conflict of interest The authors declare that they have no conflicts of interest.

Ethics approval and consent to participate Not applicable

Consent for publication Not applicable

References

1. Orini M, Nanda A, Yates M, Di Salvo C, Roberts N, Lambiase PD, Taggart P (2017) Mechano-electrical feedback in the clinical setting: Current perspectives Prog Biophys Mol Biol 130:365-375
2. Pfeiffer ER, Tangney JR, Omens JH, McCulloch AD (2014) Biomechanics of cardiac electromechanical coupling and mechanoelectric

feedback J Biomech Eng 136:021007
3. Weckström M, Tavi P, Lab MJ (2007) Mechanoelectric Transduction/Feedback: Physiology and Pathophysiology. In: Weckström M, Tavi P (eds) Cardiac Mechanotransduction. Landes Bioscience and Springer Science+Business Media, pp 48-77
4. Quinn TA, Kohl P, Ravens U (2014) Cardiac mechano-electric coupling research: fifty years of progress and scientific innovation Prog Biophys Mol Biol 115:71-75
5. Markhasin V, Nikitina L, Routkevich S, Katsnelson L, Schroder E, Keller B (2002) Effects of mechanical interaction between two rabbit cardiac muscles connected in parallel Gen Physiol Biophys 21:277-302
6. Markhasin VS, Solovyova O, Katsnelson LB, Protsenko Y, Kohl P, Noble D (2003) Mechano-electric interactions in heterogeneous myocardium: development of fundamental experimental and theoretical models Prog Biophys Mol Biol 82:207-220
7. Protsenko YL et al. (2005) Hybrid duplex: a novel method to study the contractile function of heterogeneous myocardium Am J Physiol Heart Circ Physiol 289:H2733-2746
8. Solovyova O et al. (2006) Activation sequence as a key factor in spatio-temporal optimization of myocardial function Philos Trans A Math Phys Eng Sci 364:1367-1383
9. Solovyova O et al. (2003) Mechanical interaction of heterogeneous cardiac muscle segments in silico: effects on Ca^{2+} handling and action potential Int J Bifurcat Chaos 13:3757-3782
10. Vikulova NA, Katsnelson LB, Kursanov AG, Solovyova O, Markhasin VS (2016) Mechano-electric feedback in one-dimensional model of myocardium J Math Biol 73:335-366
11. Iribe G et al. (2009) Axial stretch of rat single ventricular cardiomyocytes causes an acute and transient increase in Ca^{2+} spark rate Circ Res 104:787-795
12. Allen D, Kentish J (1988) Calcium concentration in the myoplasm of skinned ferret ventricular muscle following changes in muscle length J Physiol 407:489-503
13. Gordon AM, Regnier M, Homsher E (2001) Skeletal and cardiac muscle contractile activation: tropomyosin "rocks and rolls" News Physiol Sci 16:49-55
14. Peyronnet R, Nerbonne JM, Kohl P (2016) Cardiac Mechano-Gated Ion Channels and Arrhythmias Circ Res 118:311-329
15. Kaufmann R, Lab M, Hennekes R, Krause H (1971) Feedback interaction of mechanical and electrical events in the isolated mammalian ventricular myocardium (cat papillary muscle) Pflügers Archiv 324:100-123
16. Levine JH, Guarnieri T, Kadish AH, White RI, Calkins H, Kan JS (1988) Changes in myocardial repolarization in patients undergoing balloon valvuloplasty for congenital pulmonary stenosis: evidence for contraction-excitation feedback in humans Circulation 77:70-77
17. Taggart P et al. (1988) Monophasic action potentials at discontinuation of cardiopulmonary bypass: evidence for contraction-excitation feedback in man Circulation 77:1266-1275
18. Priebe L, Beuckelmann DJ (1998) Simulation study of cellular electric properties in heart failure Circ Res 82:1206-1223
19. Grandi E, Pasqualini FS, Bers DM (2010) A novel computational model of the human ventricular action potential and Ca transient J Mol Cell Cardiol 48:112-121
20. ten Tusscher KH, Panfilov AV (2006) Alternans and spiral breakup in a human ventricular tissue model Am J Physiol Heart Circ Physiol 291:H1088-1100
21. O'Hara T, Virag L, Varro A, Rudy Y (2011) Simulation of the undiseased human cardiac ventricular action potential: model formulation and experimental validation PLoS Comput Biol 7:e1002061
22. De Oliveira B, Rocha B, Barra L, Toledo E, Sundnes J, Weber dos Santos R (2013) Effects of deformation on transmural dispersion of repolarization using in silico models of human left ventricular wedge Int J Numer Method Biomed Eng 29:1323-1337
23. Lascano EC, Said M, Vittone L, Mattiazzi A, Mundina-Weilenmann C, Negroni JA (2013) Role of CaMKII in post acidosis arrhythmias: a simulation study using a human myocyte model J Mol Cell Cardiol 60:172-183
24. Timmermann V, Dejgaard LA, Haugaa KH, Edwards AG, Sundnes J, McCulloch AD, Wall ST (2017) An integrative appraisal of mechano-electric feedback mechanisms in the heart Prog Biophys Mol Biol 130:404-417
25. Himeno Y, Asakura K, Cha CY, Memida H, Powell T, Amano A, Noma A (2015) A human ventricular myocyte model with a refined representation of excitation-contraction coupling Biophys J 109:415-427
26. Rice JJ, Wang F, Bers DM, De Tombe PP (2008) Approximate model of cooperative activation and crossbridge cycling in cardiac muscle using ordinary differential equations Biophys J 95:2368-2390
27. Land S, Park-Holohan SJ, Smith NP, Dos Remedios CG, Kentish JC, Niederer SA (2017) A model of cardiac contraction based on novel measurements of tension development in human cardiomyocytes J Mol Cell Cardiol 106:68-83
28. Sulman T, Katsnelson LB, Solovyova O, Markhasin VS (2008) Mathematical modeling of mechanically modulated rhythm disturbances in homogeneous and heterogeneous myocardium with attenuated activity of Na^{+}-K^{+} pump Bull Math Biol 70:910-949
29. Kazbanov IV, ten Tusscher KH, Panfilov AV (2016) Effects of Heterogeneous Diffuse Fibrosis on Arrhythmia Dynamics and Mechanism Sci Rep 6:20835
30. Dutta S, Minchole A, Zacur E, Quinn TA, Taggart P, Rodriguez B (2016) Early afterdepolarizations promote transmural reentry in ischemic human ventricles with reduced repolarization reserve Prog Biophys Mol Biol 120:236-248
31. Perez Alday EA, Whittaker DG, Benson AP, Colman MA (2019) Effects of Heart Rate and Ventricular Wall Thickness on Non-invasive Mapping: An in silico Study Front Physiol 10:308
32. Vandersickel N, Watanabe M, Tao Q, Fostier J, Zeppenfeld K, Panfilov AV (2018) Dynamical anchoring of distant arrhythmia sources by fibrotic regions via restructuring of the activation pattern PLoS Comput Biol 14:e1006637
33. Zhan HQ, Xia L, Shou GF, Zang YL, Liu F, Crozier S (2014) Fibroblast proliferation alters cardiac excitation conduction and contraction: a computational study J Zhejiang Univ Sci B 15:225-242
34. Katsnelson LB, Nikitina LV, Chemla D, Solovyova O, Coirault C, Lecarpentier Y, Markhasin VS (2004) Influence of viscosity on myocardium mechanical activity: a mathematical model J Theor Biol 230:385-405
35. McDonald KS, Moss RL (1995) Osmotic compression of single cardiac myocytes eliminates the reduction in Ca^{2+} sensitivity of tension at short sarcomere length Circ Res 77:199-205
36. Wang YP, Fuchs F (1995) Osmotic compression of skinned cardiac and skeletal muscle bundles: effects on force generation, Ca^{2+} sensitivity and Ca^{2+} binding J Mol Cell Cardiol 27:1235-1244
37. Mateja RD, Greaser ML, de Tombe PP (2013) Impact of titin isoform on length dependent activation and cross-bridge cycling kinetics in rat skeletal muscle Biochim Biophys Acta 1833:804-811
38. Ait-Mou Y, Hsu K, Farman GP, Kumar M, Greaser ML, Irving TC, de Tombe PP (2016) Titin strain contributes to the Frank-Starling law of the heart by structural rearrangements of both thin- and thick-filament proteins Proc Natl Acad Sci U S A 113:2306-2311
39. Noble D, Varghese A, Kohl P, Noble P (1998) Improved guinea-pig ventricular cell model incorporating a diadic space, I_{Kr} and I_{Ks}, and length- and tension-dependent processes Can J Cardiol 14:123-134
40. Katsnelson LB, Sulman T, Solovyova O, Markhasin VS (2011) Role of myocardial viscoelasticity in disturbances of electrical and mechanical activity in calcium overloaded cardiomyocytes: mathematical modeling J Theor Biol 272:83-95
41. Izakov V, Katsnelson LB, Blyakhman FA, Markhasin VS, Shklyar TF (1991) Cooperative effects due to calcium binding by troponin and their consequences for contraction and relaxation of cardiac muscle under various conditions of mechanical loading Circ Res 69:1171-1184
42. Brixius K, Hoischen S, Reuter H, Lasek K, Schwinger RH (2001) Force/shortening-frequency relationship in multicellular muscle strips and single cardiomyocytes of human failing and nonfailing hearts J Card Fail 7:335-341

43. Gauthier C, Tavernier G, Charpentier F, Langin D, Le Marec H (1996) Functional beta3-adrenoceptor in the human heart J Clin Invest 98:556-562
44. Gwathmey JK et al. (1991) Diastolic dysfunction in hypertrophic cardiomyopathy. Effect on active force generation during systole J Clin Invest 87:1023-1031
45. Hasenfuss G, Mulieri LA, Leavitt BJ, Allen PD, Haeberle JR, Alpert NR (1992) Alteration of contractile function and excitation-contraction coupling in dilated cardiomyopathy Circ Res 70:1225-1232
46. Hasenfuss G, Mulieri LA, Blanchard EM, Holubarsch C, Leavitt BJ, Ittleman F, Alpert NR (1991) Energetics of isometric force development in control and volume-overload human myocardium. Comparison with animal species Circ Res 68:836-846
47. Holubarsch C et al. (1998) Shortening versus isometric contractions in isolated human failing and non-failing left ventricular myocardium: dependency of external work and force on muscle length, heart rate and inotropic stimulation Cardiovasc Res 37:46-57
48. Janssen PM, Lehnart SE, Prestle J, Hasenfuss G (1999) Preservation of contractile characteristics of human myocardium in multi-day cell culture J Mol Cell Cardiol 31:1419-1427
49. Mulieri LA, Hasenfuss G, Leavitt B, Allen PD, Alpert NR (1992) Altered myocardial force-frequency relation in human heart failure Circulation 85:1743-1750
50. Phillips PJ, Gwathmey JK, Feldman MD, Schoen FJ, Grossman W, Morgan JP (1990) Post-extrasystolic potentiation and the force-frequency relationship: differential augmentation of myocardial contractility in working myocardium from patients with end-stage heart failure J Mol Cell Cardiol 22:99-110
51. Pieske B et al. (1995) Alterations in intracellular calcium handling associated with the inverse force-frequency relation in human dilated cardiomyopathy Circulation 92:1169-1178
52. Pieske B et al. (1996) Diminished post-rest potentiation of contractile force in human dilated cardiomyopathy. Functional evidence for alterations in intracellular Ca2+ handling J Clin Invest 98:764-776
53. Schouten VJ, ter Keurs HE, Quaegebeur JM (1990) Influence of electrogenic Na/Ca exchange on the action potential in human heart muscle Cardiovasc Res 24:758-767
54. Schwinger RH et al. (1994) The failing human heart is unable to use the Frank-Starling mechanism Circ Res 74:959-969
55. Vahl CF, Bonz A, Timek T, Hagl S (1994) Intracellular calcium transient of working human myocardium of seven patients transplanted for congestive heart failure Circ Res 74:952-958
56. Vahl CF et al. (1997) Myocardial length-force relationship in end stage dilated cardiomyopathy and normal human myocardium: analysis of intact and skinned left ventricular trabeculae obtained during 11 heart transplantations Basic Res Cardiol 92:261-270
57. Milani-Nejad N et al. (2015) The Frank-Starling mechanism involves deceleration of cross-bridge kinetics and is preserved in failing human right ventricular myocardium Am J Physiol Heart Circ Physiol 309:H2077-2086
58. Lab MJ, Allen DG, Orchard CH (1984) The effects of shortening on myoplasmic calcium concentration and on the action potential in mammalian ventricular muscle Circ Res 55:825-829
59. Lecarpentier Y, Waldenstrom A, Clergue M, Chemla D, Oliviero P, Martin JL, Swynghedauw B (1987) Major alterations in relaxation during cardiac hypertrophy induced by aortic stenosis in guinea pig Circ Res 61:107-116
60. Lecarpentier YC, Chuck L, Housmans PR, De Clerck NM, Brutsaert DL (1979) Nature of load dependence of relaxation in cardiac muscle Am J Physiol Heart Circ Physiol 237:H455-H460
61. Brutsaert DL, De Clerck N, Goethals M, Housmans P (1978) Relaxation of ventricular cardiac muscle J Physiol 283:469-480
62. Gwathmey JK, Slawsky MT, Hajjar RJ, Briggs GM, Morgan JP (1990) Role of intracellular calcium handling in force-interval relationships of human ventricular myocardium J Clin Invest 85:1599-1613
63. Elnakish MT, Canan BD, Kilic A, Mohler PJ, Janssen PM (2017) Effects of zacopride, a moderate I_{K1} channel agonist, on triggered arrhythmia and contractility in human ventricular myocardium Pharmacol Res 115:309-318
64. Dobrunz LE, Berman MR (1994) Effect of temperature on Ca2+-dependent and mechanical modulators of relaxation in mammalian myocardium Journal of molecular and cellular cardiology 26:243-250
65. Sipido KR, Volders PG, Vos MA, Verdonck F (2002) Altered Na/Ca exchange activity in cardiac hypertrophy and heart failure: a new target for therapy? Cardiovasc Res 53:782-805
66. Weisser-Thomas J, Piacentino V, 3rd, Gaughan JP, Margulies K, Houser SR (2003) Calcium entry via Na/Ca exchange during the action potential directly contributes to contraction of failing human ventricular myocytes Cardiovasc Res 57:974-985
67. Sagawa K, Suga H, Shoukas AA, Bakalar KM (1977) End-systolic pressure/volume ratio: a new index of ventricular contractility Am J Cardiol 40:748-753
68. Josephson RK (1985) Mechanical power output from striated muscle during cyclic contraction J Exp Biol 114:493-512
69. Helmes M, Najafi A, Palmer BM, Breel E, Rijnveld N, Iannuzzi D, van der Velden J (2016) Mimicking the cardiac cycle in intact cardiomyocytes using diastolic and systolic force clamps; measuring power output Cardiovasc Res 111:66-73
70. Protsenko YL et al. (2019) Further analysis of rat myocardium contractility changes associated with a subchronic lead intoxication Food Chem Toxicol 125:233-241
71. Coppini R et al. (2013) Late sodium current inhibition reverses electromechanical dysfunction in human hypertrophic cardiomyopathy Circulation 127:575-584
72. Lou Q, Fedorov VV, Glukhov AV, Moazami N, Fast VG, Efimov IR (2011) Transmural heterogeneity and remodeling of ventricular excitation-contraction coupling in human heart failure Circulation 123:1881-1890
73. Lookin ON, Protsenko YL (2016) The kinetics of cytosolic calcium in the right ventricular myocardium of guinea pigs and rats Biophysics 61:119-132
74. Solovyova O, Vikulova N, Markhasin V, Kohl P (2003) A novel method for quantifying the contribution of different intracellular mechanisms to mechanically induced changes in action potential characteristics Lecture Notes in Computer Science 2674:8-17
75. Niederer SA, Smith NP (2007) A mathematical model of the slow force response to stretch in rat ventricular myocytes Biophys J 92:4030-4044
76. Kentish JC, Wrzosek A (1998) Changes in force and cytosolic Ca2+ concentration after length changes in isolated rat ventricular trabeculae J Physiol 506 (Pt 2):431-444
77. Lab MJ (1980) Transient depolarisation and action potential alterations following mechanical changes in isolated myocardium Cardiovasc Res 14:624-637
78. Saeki Y, Kurihara S, Hongo K, Tanaka E (1993) Alterations in intracellular calcium and tension of activated ferret papillary muscle in response to step length changes J Physiol 463:291-306
79. Kohl P, Day K, Noble D (1998) Cellular mechanisms of cardiac mechano-electric feedback in a mathematical model Can J Cardiol 14:111-119
80. Zabel M, Koller BS, Sachs F, Franz MR (1996) Stretch-induced voltage changes in the isolated beating heart: importance of the timing of stretch and implications for stretch-activated ion channels Cardiovascular Research 32:120-130
81. Grabarek Z, Grabarek J, Leavis PC, Gergely J (1983) Cooperative binding to the Ca2+-specific sites of troponin C in regulated actin and actomyosin J Biol Chem 258:14098-14102
82. Razumova MV, Bukatina AE, Campbell KB (2000) Different myofilament nearest-neighbor interactions have distinctive effects on contractile behavior Biophys J 78:3120-3137
83. Fukuda N, Wu Y, Farman G, Irving TC, Granzier H (2005) Titin-based modulation of active tension and interfilament lattice spacing in skinned rat cardiac muscle Pflugers Arch 449:449-457
84. Fukuda N, Terui T, Ohtsuki I, Ishiwata S, Kurihara S (2009) Titin and troponin: central players in the frank-starling mechanism of the heart

Curr Cardiol Rev 5:119-124
85. Landesberg A, Sideman S (1994) Mechanical regulation of cardiac muscle by coupling calcium kinetics with cross-bridge cycling: a dynamic model Am J Physiol 267:H779-795
86. Dupuis LJ, Lumens J, Arts T, Delhaas T (2016) Mechano-chemical Interactions in Cardiac Sarcomere Contraction: A Computational Modeling Study PLoS Comput Biol 12:e1005126
87. Dupuis LJ, Arts T, Prinzen FW, Delhaas T, Lumens J (2018) Linking cross-bridge cycling kinetics to response to cardiac resynchronization therapy: a multiscale modelling study Europace 20:iii87-iii93
88. Allen DG, Kurihara S (1982) The effects of muscle length on intracellular calcium transients in mammalian cardiac muscle J Physiol 327:79-94
89. Calaghan SC, White E (1999) The role of calcium in the response of cardiac muscle to stretch Progress in Biophysics and Molecular Biology 71:59-90
90. Cannell MB (2009) Pulling on the heart strings: a new mechanism within Starling's law of the heart? Circ Res 104:715-716
91. Isenberg G, Kazanski V, Kondratev D, Gallitelli MF, Kiseleva I, Kamkin A (2003) Differential effects of stretch and compression on membrane currents and [Na+]c in ventricular myocytes Prog Biophys Mol Biol 82:43-56
92. Guharay F, Sachs F (1984) Stretch-activated single ion channel currents in tissue-cultured embryonic chick skeletal muscle J Physiol 352:685-701
93. Zeng T, Bett GC, Sachs F (2000) Stretch-activated whole cell currents in adult rat cardiac myocytes Am J Physiol Heart Circ Physiol 278:H548-557
94. Healy SN, McCulloch AD (2005) An ionic model of stretch-activated and stretch-modulated currents in rabbit ventricular myocytes Europace 7 Suppl 2:128-134
95. Zhang YH, Youm JB, Sung HK, Lee SH, Ryu SY, Ho WK, Earm YE (2000) Stretch-activated and background non-selective cation channels in rat atrial myocytes J Physiol 523 Pt 3:607-619
96. Lerman BB, Engelstein ED, Burkhoff D (2001) Mechanoelectrical feedback: role of β-adrenergic receptor activation in mediating load-dependent shortening of ventricular action potential and refractoriness Circulation 104:486-490
97. Hu H, Sachs F (1997) Stretch-activated ion channels in the heart J Mol Cell Cardiol 29:1511-1523
98. Tan JH, Liu W, Saint DA (2004) Differential expression of the mechanosensitive potassium channel TREK-1 in epicardial and endocardial myocytes in rat ventricle Experimental physiology 89:237-242